PHYSICAL REVIEW B VOLUME 35, NUMBER 17 15 JUNE 1987-I

# Defect vibrational modes in germanium crystals

P. J. Lin-Chung
*Naval Research Laboratory, Washington, D.C. 20375-5000*

C. Y. Fong
*Department of Physics, University of California, Davis, California 95616*
(Received 15 October 1986)

The lattice-dynamic method is applied to a supercell to study the defect modes of Si in a Ge host crystal. The Keating potential is used to characterize the interaction between the atoms. Model calculations are performed first to compare with previous one-dimensional and Green's-function approaches. Realistic calculations of local modes for Si impurities are then carried out. Reasonable quantitative agreement with measured infrared and Raman spectra is obtained.

## I. INTRODUCTION

The lattice vibrations of pure covalent crystals are now reasonably well understood.[1] The introduction of defects into perfect group-IV crystals has two major effects: Firstly, because the translational and the inversion symmetries are broken by the presence of the defects, infrared (ir) absorption by all phonons in the diamond lattice can be induced, and the study of the one-phonon frequency spectrum by infrared measurements is then possible.[2] Careful measurements of such impurity induced one-phonon absorption spectra therefore should yield the features of the critical points in the Brillouin zone of the host crystal. Secondly, the defects may create new modes which are localized around the defect sites with frequencies split away from the bulk band of vibrational modes and which may exist either in the gap or above the maximum vibration frequency of the host system. Experimental studies on such localized modes have been performed by ir absorption and Raman scattering spectroscopies.[3] Our present theoretical study will focus on the defect-induced localized vibrational modes only.

Theoretical studies of the localized modes are relatively scarce so far. The simplest theoretical approach to the defect problem is to use the linear-chain model[3] and to calculate the local vibrational modes induced by mass defects or changes of force constants. This approach can only characterize the bond stretching modes in group-IV elemental semiconductors. The bond-bending modes involving noncentral forces cannot be accounted for in this way. The generalization to $n$-dimensional chains has been given by Rosenstock and Newell.[4] However, these results frequently have unphysical features because of the lack of coupling between the vibrations along different directions. A more realistic approach is the Green's-function method.[5] It is especially convenient to treat mass defects using this method. However, the effects of the changes in the force constants due to the presence of impurity sometimes are considered in an *ad hoc* fashion. Therefore, these two methods are useful if one is interested only in the qualitative features of the vibrational modes induced by the defects. Because theoretical studies of local modes hold special promise complementary to the electronic studies as probes of the defects, both the types and actual locations in the lattice, it is worthwhile to develop a more quantitative approach to study the local mode problems.

Recently the lattice-dynamics method combined with the supercell idea has been applied with reasonable success to amorphous silicon and hydrogenated amorphous silicon.[6,7] Based on those works, a new and useful approach is developed by us to investigate the vibrational modes of defects in tetrahedral crystals. The method prescribed here makes use of the supercell technique and the simple Keating Hamiltonian to extract quantitative results revealing both the vibrational frequencies and the details of the associated atomic motions. The Keating potential is chosen because it is short ranged and it is expected to produce the high-frequency localized modes in the same degree of accuracy as the bulk optical phonons and longitudinal acoustic phonons. In contrast to previous approaches, this method provides a more realistic model of the effects of introducing defects in tetrahedral crystals because of the proper inclusion of the angular forces and the atomic relaxations.

In this calculation, a large unit cell with 50—60 atoms is constructed from unit cells of the host crystal. Some of the host atoms are substituted by impurity atoms. Distortions induced by the introduction of the defects are determined by a realistic potential energy. After the new equilibrium positions of the atoms are determined, the same potential then is used to calculate the eigenvalues and eigenvectors of the normal vibrational modes. The advantages of using this scheme as compared to the linear chain and the Green's-function method are the following: (i) Both mass defects and the changes of force constants can be incorporated easily. (ii) Local distortions around the defects are included. This is a unique feature for this scheme. (iii) Detailed information such as the eigenvectors enables us to identify the symmetries of the local modes and to determine the selection rules for ir or Raman transitions. (iv) The effects of individual defects and the effects of the interactions between defects can be investigated if the supercell is large enough. (v) Atoms away from the defects retain the motions in the normal

 

modes similar to those in host crystal because of the periodicity. This makes the analysis of the resonance modes and the local modes relative to the normal modes of the perfect system more meaningful.

The present work utilizes the above scheme to study in general defect-induced vibrational modes. We separate the effects of changes in the defect mass, in bond-stretching force, in bond-bending force constant, and in the bond length in our model investigations. We then study the local modes induced by introducing Si impurities in Ge crystal. In Sec. II the method will be presented. Results for local modes and resonance modes induced by different defects in the model studies and the results of realistic single substitutional Si and Si-Si complex defects in Ge crystal will be discussed in Sec. III.

## II. METHOD OF CALCULATION

In order to study the diamond lattice with defects, we construct a supercell which is a simple cubic unit cell containing 64 basis atoms. The lattice constant of the supercell is $2a$ where $a$ is the lattice constant of the host crystal. If no defect is present, this cell is identical to a combination of eight unit cells of a diamond lattice. Defects are situated near the center of the supercell. Such a supercell extends periodically to form the perturbed crystal. As will be shown later, with such a large unit cell, the separation between defects in different cells is greater than the extent of the local mode wave functions so that interactions between the defects in separate cells may be neglected. Thus the present supercell approach is adequate for studies of defects.

The Keating potential[8] has been used widely to study the elastic and static properties of covalent semiconductors because it involves only two parameters yet it preserves the rotational invariant condition of the crystal.[8–10] This potential is closely related to the valence-force-field potentials which have been used for the calculations of the phonon-dispersion relations in group-IV crystals.[11–13] The results have shown good agreement with experiments except for the transverse acoustic (TA) branches which lie at too high frequencies. Because the Keating potential is short-ranged it dominates the optical phonons (LO and TO) and longitudinal acoustic phonons (LA), we choose to use this simple potential here to investigate the high-frequency localized modes induced by impurity defects.

The Keating potential at an atom "0" is expressed in the following form.

$$U_0=\sum_{i=1}^{4}\frac{3\alpha_{0i}}{8d_i^2}[(\mathbf{x}_{i0}\cdot\mathbf{x}_{i0})-d_i^2]^2 + \sum_i \sum_{j\,(>i)} \frac{3\beta_{0ij}}{8d_{ij}^2}\left[(\mathbf{x}_{i0}\cdot\mathbf{x}_{j0})+\frac{d_{ij}^2}{3}\right]^2, \quad (1)$$

where $\alpha_{0i}$ is the bond-stretching force constant between atoms 0 and $i$. $d_i$ is the equilibrium bond length between the two atoms. $x_{i0}$ is the bond vector from atom 0 to atom $i$. $\beta_{0ij}$ is the bond-bending force constant between the bonds centered at the atom 0. $d_{ij}^2$ is the product of $d_i$ and $d_j$.

When impurity atoms are present, the force-constant parameters and the equilibrium bond lengths between a given pair of atoms are allowed to change and are determined by the following procedure: (i) If $i$, $j$, and 0 are atoms of the same species, we use the corresponding values of $\alpha$, and $d$ given by Martin in his work of elastic properties of group-IV materials.[9] (ii) If 0 and $i$ are atoms of the same kind while atom $j$ is of different kind, we first average the $\beta$ and $d$ values of Martin for the bond 0—$j$. Then we average again for the $\beta_{0ii}$ and $\beta_{0jj}$ values to get $\beta_{0ij}$. (iii) If 0 and $i$ are atoms of different kind, we average the values for 0-0 and $i$-$i$ to get $\alpha_{0i}$ and $\beta_{0ii}$ and then follow the same procedure in (ii) to get $\beta_{0ij}$.

Initially, the impurity atoms are assumed to be separated from their neighbors by the ideal bond length of the pure crystal which may not be the equilibrium separation between them. Due to the fact that the force on the nearest neighbors of the impurity are not zero for such a separation, relaxation of atomic positions occurs. We use the Keating potential to relax the lattice until the total strain energy calculated from the potential is a minimum. The relaxation becomes more pronounced and has more profound effects on the local modes when the size of the impurity deviates more from that of the host atoms. With these new relaxed atomic positions, we then set up the dynamical matrix for the vibrational-mode calculation.

One of the important features of the supercell scheme is that it can provide the eigenvector of each vibrational mode by diagonalizing the dynamical matrix. To compare with the ir and Raman spectra, only the zone center ($k=0$) modes are considered. From these eigenvectors it is possible to identify the symmetry of each mode and to obtain the detailed vibrational amplitudes of the local modes at each atomic position. Based upon the symmetries of the modes, a comparison of the calculated results with the features in the infrared and the Raman spectra can be made.

## III. RESULTS AND DISCUSSIONS

We first made model calculations to examine in detail the effects of variations in the mass, $m'$, in the bond stretching force constant $\alpha'$, and in the bond-bending parameter, $\beta'$, of the defect on the vibrational spectrum of Ge crystal. For convenience, we define $\varepsilon_m=1-m'/m$, $\varepsilon_\alpha=1-\alpha'/\alpha$, and $\varepsilon_\beta=1-\beta'/\beta$. Then we carried out calculations of the local vibrational modes associated with a substitution Si impurity and pairs of substitutional Si atoms in Ge. For the case of the pair complex, both configurations in which the atoms are situated at first-nearest-neighbor (1NN) sites and at second-near-neighbor (2NN) positions were considered.

### A. Pure Ge and Si crystals

In order to check the supercell scheme and the parameters used, we first examine the cases of pure Ge and Si crystals. The force constants for Ge and Si are taken from Martin's calculations.[9] Our calculated phonon spectrum for pure Ge and Si give good agreement with experiment[14] except for the transverse acoustic mode near the

zone boundary as expected. The zone-center optical phonons are at 304 and 518 $cm^{-1}$ as compared with the measured value of 304 and 520 $cm^{-1}$ for Ge and Si, respectively. The TA mode frequencies are high (the TA mode at point $X$ for Ge is 137 instead of 80 $cm^{-1}$) because the shear force has not been properly accounted for in the Keating potential. However, this is not expected to have a significant effect on the high-frequency local modes which are the focus of our study.

Previously, several theoretical calculations for the phonon-dispersion relations of Ge have been carried out employing lattice-dynamical models[15-16] which combined the bond charge effect with the valence force field and which introduced more disposable parameters. Although those models produce better agreement with the observed TA modes, they become extremely difficult to handle in the supercell calculation. This difficulty arises in the presence of defects or defect complexes because, in addition to the changes in the bond lengths, the charges have also redistributed among the impurities and the nearby host atoms. As a result, the scheme to scale the force constants becomes more complicated than the one provided in Ref. 17 in order to obtain better agreement with the TA modes. Fortunately in comparison with those theoretical calculations, the simple two-parameter model used here produces comparably reasonable results in pure Ge crystal for the high-frequency vibrational modes which are in the spectra region of our interest. A comparison of our calculated values of phonon frequencies at high-symmetry points with the measured values given in Ref. 14 is made in Table I.

Our calculated phonon spectrum histogram for Ge in Fig. 1(a) resembles the results given by Nilin and Nilsson.[18] The TA branch, however, again occurs at higher position than the experimental results. Since later on we will study defect-induced vibrational modes which are related to the critical points of the phonon spectrum of pure crystal, we also display in Fig. 1(b) the contribution to the spectrum from the $k=0$ eigenvalues of the supercell. The $k=0$ of the Brillouin zone (BZ) of the supercell involves the high-symmetry points $\Gamma$, $L$, $X$, $W$, $\Delta$, and $\Sigma$ of the diamond Brillouin zone (DBZ) folded into the new BZ. Critical points often occur at high-symmetry points of the DBZ. These eigenvalues of the high-symmetry points have been listed in Table I, and several of them are indicated by arrows in Fig. 1(b).

### B. Effects of mass defects and of changes in the force constants in Ge

We first consider an isotopic substitutional impurity with a mass defect $\epsilon_m$ bound to its neighbors by the same force constants as the host Ge crystal. The $\epsilon_m=0$ case is the pure Ge case given in Fig. 1(b). For $\epsilon_m<0$, a negative mass defect, no local mode exists. However, many resonance modes appear. We show in Fig. 1(c) the corresponding $k=0$ phonon histogram for a mass defect equal to $-2$. The prominant resonance modes are indicated by arrows there. The defect atom contributes significantly only at these resonant modes. The appearance of these resonance modes can be understood qualitatively. Because the local contribution of the defect atom should be characterized by the modes of short wavelengths, the modes at $\Gamma$ point are not influenced. Following Ref. 17,

TABLE I. Calculated phonon frequencies at high-symmetry points of the reduced Brillouin zone for pure Ge crystal. (The numbers in parentheses represent the measured values reported in Ref. 14.)

| $(a/2)(k_x,k_y,k_z)$ | $\omega$ ($cm^{-1}$) | | | | | |
|---|---|---|---|---|---|---|
| $\Gamma$ | $\Gamma_{15}$ | $\Gamma_{15}$ | | | | |
| (0,0,0) | 0 | 304 | | | | |
| | (0) | (304) | | | | |
| $X$ | $X_3$ | $X_1$ | | $X_4$ | | |
| (1,0,0) | 137.4 | 237.5 | | 268 | | |
| | (80) | (240) | | (275) | | |
| $L$ | $L_3$ | $L_2$ | $L_1$ | $L_3$ | | |
| (0.5,0.5,0.5) | 91 | 228 | 238.7 | 289.7 | | |
| | (63.33) | (222) | (245) | (290) | | |
| $\Delta$ | $\Delta_5$ | $\Delta_1$ | $\Delta_2'$ | $\Delta_5$ | | |
| (0.5,0,0) | 95 | 145 | 286 | 291 | | |
| | (70) | (139) | (280.7) | (293) | | |
| $W$ | $W_2$ | $W_1$ | $W_2$ | | | |
| (1,0.5,0) | 160 | 214.5 | 278 | | | |
| | (114) | (207) | (278.7) | | | |
| $\Sigma$ | $\Sigma_4$ | $\Sigma_3$ | $\Sigma_1$ | $\Sigma_3$ | $\Sigma_2$ | $\Sigma_1$ |
| (0.5,0.5,0) | 75 | 103 | 153 | 242 | 287 | 289 |
| | (78) | (111) | (165) | (247) | (282) | (289) |

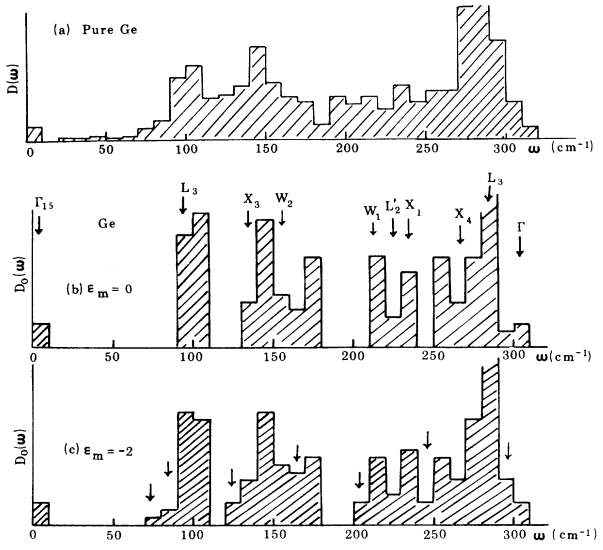


FIG. 1. (a) The calculated phonon frequency spectrum, $D(\omega)$, for pure Ge crystal. (b) The $k=0$ phonon frequency histogram, $D_0(\omega)$, for Ge supercell containing no defect ($\varepsilon_m=0$). (c) The $k=0$ phonon frequency histogram, $D_0(\omega)$, for Ge supercell containing impurities with mass defects $\varepsilon_m=-2$. The arrows in (b) represent the phonon frequencies of the modes corresponding to the symmetry points in the reduced Brillouin zone. The arrows in (c) represent the positions of the resonance modes induced by the defect.

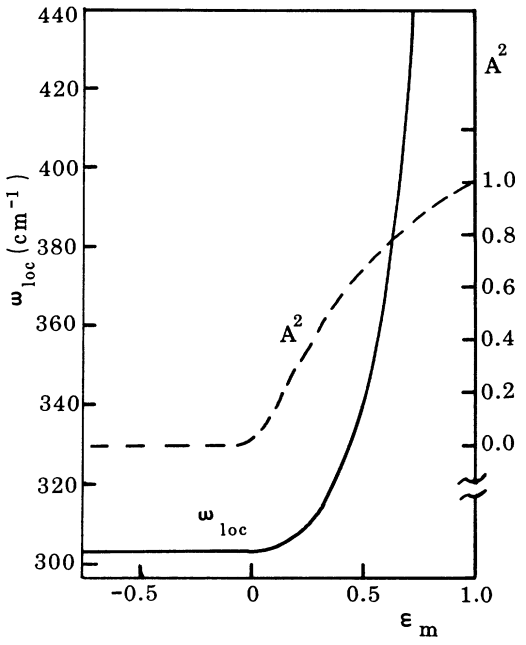


FIG. 2. The local mode frequency, $\omega_{\rm loc}$, solid curve, and the vibrational amplitude of the impurity, $A^2$, dashed curve, as functions of the mass defect parameter $\varepsilon_m$.

we approximately divide the spectrum into regions contributed from TA, LA, LO, and TO branches, respectively, the dividing points are at 110, 165, 240, and 310 $\rm cm^{-1}$. The four arrows at $\omega > 160$ $\rm cm^{-1}$ correspond to the modifications in one each of LA, LO and two of the TO regions. In the TA mode region ($\omega < 130$ $\rm cm^{-1}$), there are more changes. These vibrational modes can be characterized as bond-bending motions. The defect can participate in many bending motions with respect to the neighboring Ge atoms. Therefore, more resonance modes are found in this region. For $\varepsilon_m > 0$, positive mass defect, (light atom substitution) a triply degenerate local vibrational mode appears above the host-crystal phonon spectrum. The frequency $\omega_{\rm loc}$ increases rapidly with increasing $\varepsilon_m$ as shown in Fig. 2. The vibrational amplitude $|A|$ of the defect atom also increases drastically as the atom becomes lighter. These results agree qualitatively with the Green's-function calculations using a Debye spectrum.[19]

We also have examined the squared amplitude of a defect atom relative to that of an atom in pure Ge as a function of frequency. The overall features of the variation agree with Green's-function calculation for a Debye spectrum[19] as shown in Fig. 3. However, quantitatively they are different. We found that for $\varepsilon_m=-2$ a large enhancement of the vibrational amplitude at $\omega=0.26\omega_L$ signifies a resonant mode, whereas the results of Ref. 19 (dashed curve in Fig. 3) show a peak at $\omega=0.35\omega_L$. For the case of $\varepsilon_m > 0$ and $\omega < \omega_L$, the vibrational amplitude of the defect atom becomes smaller than that of an atom in a perfect lattice. Here $\omega_L$ is the maximum phonon frequency in Ge.

The cases when only the bond-stretching parameter or the bond-bending parameter is allowed to change are now discussed. The calculated results given in Fig. 4 show that local modes exist for negative $\varepsilon_\alpha$ (larger force constant). The vibrational amplitude of the defect atom and the $\omega_{\rm loc}(\varepsilon_\alpha)$ increase as $\varepsilon_\alpha$ becomes more negative. In the range of $-1 < \varepsilon_\beta < 0$, the $\omega_{\rm loc}(\varepsilon_\beta)$ changes less than 0.01%, and therefore the effect is negligible. The effects of changes in bond-stretching and the bond-bending force

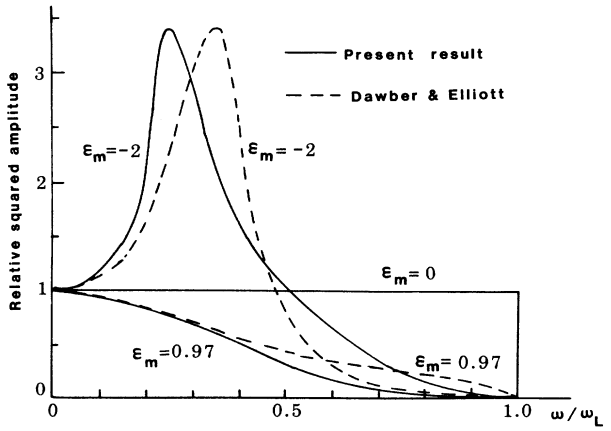


FIG. 3. The squared amplitude of a defect atom relative to that of an atom in Ge crystal, as a function of $\omega/\omega_L$ for various values of $\varepsilon_m$. Dashed curves are obtained from Ref. 19.

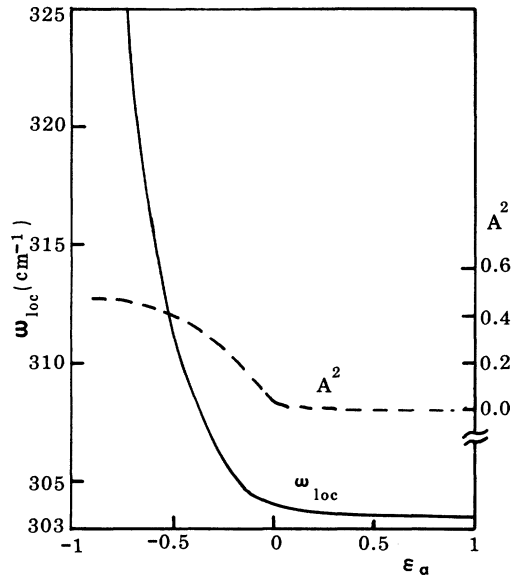


FIG. 4. The local model frequencies, $\omega_{loc}$, solid curve, and the vibrational amplitudes of the impurity, $A^2$, dashed curve, as functions of bond-stretching defect parameters $\varepsilon_\alpha$.

constants are not as significant as changes in the mass defect. This may be due to our averaging process in getting effective force constants. In fact, the actual change in the averaged force constant is not as large as indicated by the change of $\varepsilon_\alpha$. On the other hand, the mass defect does not involve averaging.

### C. Isolated Si impurity in Ge crystal

With an impurity Si atom present in the Ge crystal, the force-constant parameters between the impurity and the host atoms or between the impurities themselves are determined using the parameters calculated by Martin[9] for the pure Si and pure Ge combined with our interpolation scheme discussed in Sec. II. The final values we used in this calculation are listed in Table II.

When an isolated Si impurity substitutes for a Ge atom, the 1NN Ge atoms surrounding the Si are found to relax inward and the bond lengths are shortened by 2.8%. The second-nearest-neighbor (2NN) atoms relax less than 0.04%. The strain energy per supercell is reduced by 0.02% after relaxation. As expected for a light mass defect, a threefold degenerate vibrational mode appears at 412.8 cm$^{-1}$. It is a localized mode which characterizes essentially the vibration of the Si atom against its 1NN Ge atoms. The ratio of the vibrational amplitude of the Si to the averaged amplitude of the 1NN atoms and to that of the 2NN atoms is 0.9:0.2:0.02. The distant atoms are essentially motionless. This is consistent with the picture that wavelike motions of the Ge atoms are not possible at frequencies which lie above the optic-phonon band of pure Ge. It also justifies the fact that the defects in different cells are effectively not interacting.

TABLE II. Force-constant parameters and equilibrium bond lengths used in this calculation

| 0 | i | j | $\alpha_{0i}$ ($10^3$ dyn/cm) | $\beta_{0ij}$ ($10^3$ dyn/cm) | $d_{ij}$ (Å) |
|---|---|---|---|---|---|
| Si | Si | Si | 48.50 | 13.81 | 2.351 |
| Ge | Ge | Ge | 38.67 | 11.35 | 2.449 |
| Si | Ge | Ge | 43.59 | 12.58 | 2.400 |
| Si | Si | Ge | 48.50 | 13.20 | 2.375 |
| Ge | Si | Si | 43.59 | 12.58 | 2.400 |
| Ge | Ge | Si | 38.67 | 11.97 | 2.424 |

From symmetry arguments, the odd-symmetry modes appear in the infrared absorption spectrum and the even-symmetry modes appear in the Raman spectrum. Being $t_1^+$ symmetry, the mode discussed above should be observed by Raman scattering spectrum. The observed Raman feature[20] and the neutron scattering feature[21] near 400 cm$^{-1}$ may correspond to this mode.[20] Also Cosand and Spitzer observed an optical-absorption band with a small cross section at this frequency.[22] They attributed this absorption to possible small charges associated with Si impurity which is determined by the short-range effect in covalent crystals. As we shall point out, this ir structure may be associated with Si-Si complex defect.

The earlier results of Dawber and Elliott using a Debye model yield a local mode at 392 cm$^{-1}$ when the Debye frequency was set equal to the Ge zone-center optic-phonon frequency.[19] Our results agree reasonably well with theirs.

Shen and Cardona reported the observation of several mass defect quasibound vibrational states and impurity induced one-phonon peaks in the far-infrared absorption spectra of Ge samples which were lightly alloyed with Si.[23] They also interpreted their data with a mass defect Green's-function calculation based on the density of phonon states of pure Ge from a bond charge model.[16] In Fig. 5(a) we display our $k=0$ phonon histogram for isolated Si in Ge. In comparison with Fig. 1(b), two resonances appear in the TA region and three resonances appear at higher frequencies. They are indicated by arrows.

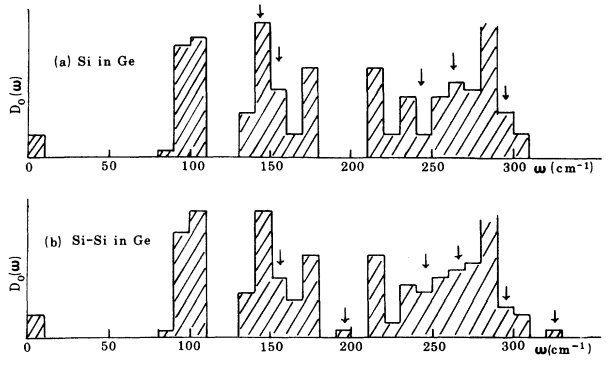


FIG. 5. (a) $k=0$ phonon frequency histogram, $D_0(\omega)$, for a Ge supercell with one Si impurity atom. (b) $k=0$ phonon frequency histogram, $D_0(\omega)$, for Ge supercell with Si-Si (1NN) impurity complexes.

The two resonances in the TA branch at 150 $cm^{-1}$ correspond to the observed large peaks at 122 $cm^{-1}$ in Ref. 23. The quantitative disagreement arises from the high TA branch obtained in the calculation. The three resonances at the LO (245 $cm^{-1}$) and TO (280 $cm^{-1}$) regions are consistent with the structure observed at 244 and 280 $cm^{-1}$ in Ref. 23. This suggests that the simple Keating's potential works well except in the TA region.

### D. Si-Si (1NN) impurity complex in Ge crystal

As shown in Fig. 6(a), in this configuration the two Si atoms are introduced substitutionally at 1NN distance along [111] direction. The symmetry is reduced to $D_{3d}$. More new modes localized about the pair of impurities occur at frequencies above the vibrational spectrum of the pure Ge crystal. The modes are listed in Table III. The symmetry of each mode and the available data measured by Raman ($R$) or infrared (ir) experiments are also listed in this table.

We find that the two Si atoms relax and move toward each other shortening the bond length by 3.05% (i.e., shorter than the ideal bond length). The 1NN Ge atoms follow the Si atoms and move toward the Si-Si complex. New bond lengths between Si and 1NN Ge atom and between two 1NN Ge atoms decrease by 0.8% and 1.43%, respectively, with respect to the unrelaxed bond length. The displacements of the Ge atoms which are 2NN of the Si atoms are negligible. Therefore, in effect, the bond length between the 1NN and the 2NN Ge atoms has increased by 0.67%. The strain energy after relaxation decreases by 0.06% per supercell.

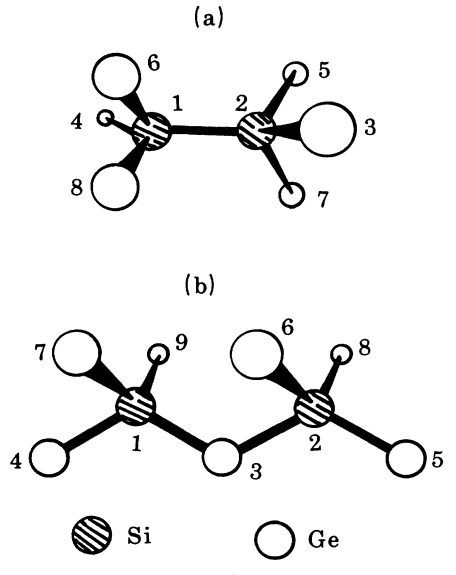


FIG. 6. The positions of the Si-Si defect complexes and their neighboring Ge atoms in the Si-Si (1NN) configuration (a), and in the Si-Si (2NN) configuration (b). The solid circles denote the Si atoms. Open circles denote the Ge atoms. In (a), the line joining 1→2 is in [111] direction, 3→5 and 8→4 are in [110] direction. In (b), atoms 1, 2, 3, 4, and 5 are all on a (011) plane. 1→2 and 4→3→5 are in [011] direction; 1→3 and 2→5 are along [111] direction.

TABLE III. Calculated localized modes associated with defects in the Ge crystal. (Numbers in parentheses represent experimentally observed values. $R$ and ir denote Raman active or infrared active.)

| Defect | Local model ($cm^{-1}$) | Symmetry |
|---|---|---|
| Si | 412.8(389) | $T_1^+$ ($R$) |
| Si-Si (1NN) | 495.24(476) | $A_1^+$ ($R$) |
| $D_{3d}$ | 430.97(448) | $E_1^+$ ($R$) |
| | 400.97(389) | $E_1^-$ (ir) |
| | 325.45 | $A_1^-$ (ir) |
| Si-Si (2NN) | 420.63 | $A_2$ (ir) |
| $C_{2v}$ | 418.19 | $A_1$ ($R$) |
| | 413.78 | $A_4$ (ir) |
| | 412.61 | $A_3$ ($R$) |
| | 408.81 | $A_1$ (ir) |
| | 407.65 | $A_2$ (ir) |

The highest-frequency mode at 495.24 $cm^{-1}$ is a molecular type of vibration. The two Si atoms vibrate with opposite phases along [111] direction while each of the 1NN Ge atoms moves along one of the [110], [101], and [011] directions with an amplitude an order of magnitude smaller than that of the impurity atoms.

The 430.97-$cm^{-1}$ mode is twofold degenerate and is also Raman active. The two Si atoms vibrate in opposite directions but perpendicular to the [111] direction. As for the three 1NN Ge atoms next to each Si atom, two of them vibrate with amplitude one-fifth while the other has amplitude one-tenth of that of the Si atoms. More distant atoms do not participate in this mode. The 495.24 and the 430.97 $cm^{-1}$ modes are compared favorably with the measured lines at 476 and 448 $cm^{-1}$ in Ref. 20.

The 400.97-$cm^{-1}$ mode is twofold degenerate but is ir active. Unlike the case of the 430.97 mode, the two Si atoms move in the same direction which is perpendicular to [111] direction. The amplitudes and the directions of vibration of the 1NN Ge atoms, however, are the same as the corresponding values for the 430.97 mode. The dipole moment is mainly due to the asymmetry of the charges at the Ge atoms. The asymmetry should not be large yet it can couple weakly to the ir radiation. Therefore it is suggested here that the experimentally observed ir absorption near 389 $cm^{-1}$ (Ref. 22) may correspond to this mode. Further experimental studies of the symmetry of this vibration can provide a definitive assignment of this observed peak as being either to the Si-Si complex or to the isolated Si local mode.

Another ir active mode induced by the Si-Si complex is at 325.45 $cm^{-1}$. This mode is less localized because the vibration involves the 2NN Ge of the Si-Si pair. The amplitude ratio of the vibrations of Si, 1NN Ge and 2NN Ge is 1:0.7:0.1. The two Si atoms and the 2NN Ge atoms vibrate in the same direction along [111]. The three Ge atoms at 1NN of each Si atom vibrate along [011], [101],

TABLE IV. The relative vibration direction ($D$) and relative amplitude ($A$) of vibration of each atom in the local modes of Si-Si (2NN) complex. [The labels of the atoms follow those given in Fig. 6(b).]

| Atom \ Local mode ($cm^{-1}$) | 420.63 | | 418.19 | | 413.78 | | 412.61 | | 408.81 | | 407.65 | |
|---|---|---|---|---|---|---|---|---|---|---|---|---|
| | $D$ | $A$ | $D$ | $A$ | $D$ | $A$ | $D$ | $A$ | $D$ | $A$ | $D$ | $A$ |
| 1 | [122] | $A$ | [$\bar{2}$11] | $A$ | [01$\bar{1}$] | $A$ | [01$\bar{1}$] | $A$ | [$\bar{1}\,\bar{1}\,\bar{1}$] | $A$ | [4$\bar{1}\,\bar{1}$] | $A$ |
| 2 | [$\bar{1}$22] | $A$ | [$\bar{2}\,\bar{1}\,\bar{1}$] | $A$ | [01$\bar{1}$] | $A$ | [0$\bar{1}$1] | $A$ | [$\bar{1}$11] | $A$ | [$\bar{4}\,\bar{1}\,\bar{1}$] | $A$ |
| 3 | [0$\bar{1}\,\bar{1}$] | $0.5A$ | [100] | $0.1A$ | [0$\bar{1}$1] | $0.2A$ | | 0 | [100] | $0.5A$ | [0$\bar{1}\,\bar{1}$] | $0.05A$ |
| 4 | [1$\bar{2}\,\bar{2}$] | $0.2A$ | [1$\bar{1}\,\bar{1}$] | $0.3A$ | [0$\bar{1}$1] | $0.1A$ | [0$\bar{1}$1] | $0.1A$ | [011] | $0.2A$ | [$\bar{1}$11] | $0.2A$ |
| 5 | [$\bar{1}\,\bar{2}\,\bar{2}$] | $0.2A$ | [111] | $0.3A$ | [0$\bar{1}$1] | $0.1A$ | [01$\bar{1}$] | $0.1A$ | [0$\bar{1}\,\bar{1}$] | $0.2A$ | [111] | $0.2A$ |
| 6 | [4$\bar{1}\,\bar{5}$] | $0.1A$ | [32$\bar{1}$] | $0.2A$ | [$\bar{1}\,\bar{1}$1] | $0.3A$ | [11$\bar{1}$] | $0.3A$ | [10$\bar{1}$] | $0.2A$ | [21$\bar{1}$] | $0.2A$ |
| 7 | [$\bar{4}\,\bar{5}\,\bar{1}$] | $0.1A$ | [31$\bar{2}$] | $0.2A$ | [$\bar{1}$11] | $0.3A$ | [$\bar{1}$11] | $0.3A$ | [110] | $0.2A$ | [$\bar{2}\,\bar{1}$1] | $0.2A$ |
| 8 | [$4\bar{5}\,\bar{1}$] | $0.1A$ | [3$\bar{1}$2] | $0.2A$ | [1$\bar{1}$1] | $0.3A$ | [$\bar{1}\,\bar{1}\,\bar{1}$] | $0.3A$ | [1$\bar{1}$0] | $0.2A$ | [2$\bar{1}$1] | $0.2A$ |
| 9 | [$\bar{4}\,\bar{1}\,\bar{5}$] | $0.1A$ | [3$\bar{2}$1] | $0.2A$ | [1$\bar{1}$1] | $0.3A$ | [1$\bar{1}$1] | $0.3A$ | [101] | $0.2A$ | [$\bar{2}\,\bar{1}\,\bar{1}$] | $0.2A$ |

[110] directions, respectively. This mode has not been observed experimentally yet.

The $k=0$ phonon frequency histogram for Si-Si in Ge is displayed in Fig. 5(b). In addition to the resonances which also appear in Fig. 5(a), a localized mode at 325.45 $cm^{-1}$ occurs just above the $\omega_L$ of pure Ge. The other localized modes at frequencies higher than 350 $cm^{-1}$ are not shown in Fig. 5.

### E. Si-Si (2NN) impurity complex in Ge crystal

When the two Si impurities are separated by 2NN distance, [Fig. 6(b)], the impurities do not move during relaxation whereas the surrounding Ge atoms move toward the Si atoms. The bond lengths between Si and two of the 1NN Ge atoms are shortened by 1.4% and those between Si and other 1NN atoms are shortened by 0.9%. The strain energy is decreased by 0.03% after relaxation. In comparison with the Si-Si (1NN) configuration, the strain energy in this configuration is lower by 1%.

Since in this defect configuration the interaction between the two Si atoms comes indirectly from the bond-bending part, it is weaker than that in the previous configuration. The localized modes therefore can be thought of as perturbed modes of isolated Si. Indeed, we find that the calculated local modes in this configuration cluster around the mode induced by an isolated Si impurity. The six nondegenerate modes are summarized in Table III. The vibrational patterns for the modes are quite different from those in the previous cases because of the geometrical difference in the environment. As shown in Fig. 6(b), the two Si atoms have seven Ge atoms as their 1NN. One of them is the common 1NN ($Cnn$) of both Si atoms. The plane containing both Si atoms (nos. 1 and 2), the $Cnn$ (no. 3), and the two other 1NN (nos. 4 and 5) is the (011) plane. Two 1NN atoms (nos. 6 and 7) lie one layer above and the other two 1NN (nos. 8 and 9) lie one layer below this plane.

The 413.78- and the 412.61-$cm^{-1}$ modes, which are the splittings of the 412.8-$cm^{-1}$ isolated Si vibration mode, involve the vibration of the no. 1 and the no. 2 Si atoms perpendicular to the (011) plane in the same and opposite directions, respectively. The vibration of the Si atoms in the four other local modes are all in the (011) plane. The detailed relative vibration direction and amplitude of each atom labeled in Fig. 6(b) is listed in Table IV for each local mode. The more distant atoms do not move in these modes.

### F. Summary

In summary, we have applied the scheme of combining the lattice-dynamic method and the supercell approach to investigate defect-induced vibrational modes in Ge crystal. A Keating potential is used. Model calculations of defect-induced modes due to mass defects or changes in the force constants $\alpha$ or $\beta$ were made. Results were compared with those obtained by the Green's-function method. Correlations of the changes in the TA, LA, LO, and TO modes due to the mass defect have been discussed. We then specifically examined the Si impurity and Si-Si pair defects in Ge. The modes induced by the pair defect with Si-Si in 1NN agree well with experimentally measured Raman lines. The Raman-active modes due to a single Si defect and the ir-active modes due to a pair Si-Si 1NN are assigned tentatively to the measured Raman line and a weak ir line. Further experiment is needed to discriminate our assignments. There are six lines due to Si-Si 2NN pair defect, but as yet there is no experimental data relating to them. Better experimental resolution is needed to find these lines.

## ACKNOWLEDGMENT

The work of P.J.L. was supported in part by an Office of Naval Research (ONR) contract.

[1]See, for example, R. Loudon, Proc. Phys. Soc. **84**, 379 (1964).
[2]A. S. Barker, Jr. and A. J. Sievers, Rev. Mod. Phys. **47**, Suppl. 2, 81, (1975), and references quoted there.
[3]A. A. Maradudin, E. W. Montroll, G. H. Weiss, and I. P. Ipatova, *Theory of Lattica Dynamics in the Harmonic Approximation* (Academic, New York, 1971), p. 438.
[4]H. B. Rosenstock and G. F. Newell, J. Chem. Phys. **21**, 1607 (1953).
[5]See the review by R. J. Elliott, J. A. Krumhansl, and P. L. Leath, Rev. Mod. Phys. **46**, 465 (1974).
[6]M. F. Ross, C. M. Perlor, C. Y. Fong, and L. Guttman, J. Non-Cryst. Solids **59& 60**, 209 (1983).
[7]K. Winer and F. Wooten, J. Non-Cryst. Solids **59& 60**, 193 (1983).
[8]P. N. Keating, Phys. Rev. **145**, 637 (1966).
[9]R. M. Martin, Phys. Rev. B **1**, 4005 (1970).
[10]J. Noolandi, Phys. Rev. B **10**, 2490 (1974).
[11]H. L. McMurray, A. W. Solbrig, J. K. Boyter, and C. Noble, J. Phys. Chem. Solids **28**, 2359 (1967).
[12]R. Tubino, L. Piseri, and G. Zerbl, J. Chem. Phys. **56**, 1022 (1972).
[13]A. W. Solbrig, J. Phys. Chem. Solids **32**, 1761 (1971).
[14]G. Nilsson and G. Nelin, Phys. Rev. B **3**, 364 (1971).
[15]G. Nelin, Phys. Rev. B **10**, 4331 (1974).
[16]W. Weber, Phys. Rev. B **15**, 4789 (1977).
[17]A. Goldberg, M. El-Batanouny, and F. Wooten, Phys. Rev. B **26**, 6661 (1980).
[18]G. Nelin and G. Nilsson, Phys. Rev. B **5**, 3151 (1972).
[19]P. G. Dawber and R. J. Elliott, Proc. R. Soc. (London), Ser. A **273**, 222 (1963).
[20]D. W. Feldman, M. Ashkin, and J. H. Parker, Jr., Phys. Rev. Lett. **17**, 1209 (1966).
[21]N. Wakabayashi, R. M. Nicklow, and H. G. Smith, Phys. Rev. B **4**, 2558 (1971).
[22]A. E. Cosand and W. J. Spitzer, J. Appl. Phys. **42**, 5241 (1971).
[23]S. C. Shen and M. Cardona, Solid State Commun. **36**, 327 (1980).